A receptor-based model for dopamine-induced fMRI signal

Joseph B. Mandeville [a,*], Christin Y.M. Sander [b], Bruce G. Jenkins [a], Jacob M. Hooker [a], Ciprian Catana [a], Wim Vanduffel [a], Nathaniel M. Alpert [c], Bruce R. Rosen [a], Marc D. Normandin [c]

[a] Athinoula A. Martinos Center for Biomedical Imaging, Massachusetts General Hospital, Charlestown, MA, USA
[b] Electrical Engineering and Computer Science, Massachusetts Institute of Technology, Cambridge, MA, USA
[c] Division of Nuclear Medicine, Massachusetts General Hospital, Boston, MA, USA

ARTICLE INFO

ABSTRACT

This report describes a multi-receptor physiological model of the fMRI temporal response and signal magnitude evoked by drugs that elevate synaptic dopamine in basal ganglia. The model is formulated as a summation of dopamine's effects at D1-like and D2-like receptor families, which produce functional excitation and inhibition, respectively, as measured by molecular indicators like adenylate cyclase or neuroimaging techniques like fMRI. Functional effects within the model are described in terms of relative changes in receptor occupancies scaled by receptor densities and neuro-vascular coupling constants. Using literature parameters, the model reconciles many discrepant observations and interpretations of pre-clinical data. Additionally, we present data showing that amphetamine stimulation produces fMRI inhibition at low doses and a biphasic response at higher doses in the basal ganglia of non-human primates (NHP), in agreement with model predictions based upon the respective levels of evoked dopamine. Because information about dopamine release is required to inform the fMRI model, we simultaneously acquired PET ^{11}C-raclopride data in several studies to evaluate the relationship between raclopride displacement and assumptions about dopamine release. At high levels of dopamine release, results suggest that refinements of the model will be required to consistently describe the PET and fMRI data. Overall, the remarkable success of the model in describing a wide range of preclinical fMRI data indicate that this approach will be useful for guiding the design and analysis of basic science and clinical investigations and for interpreting the functional consequences of dopaminergic stimulation in normal subjects and in populations with dopaminergic neuroadaptations.

© 2013 Elsevier Inc. All rights reserved.

Introduction

Many pharmacological and natural stimuli elevate synaptic levels of dopamine (DA) and elicit functional responses in flow and metabolism that are measurable using non-invasive neuroimaging methods within the DA-rich basal ganglia. However, basic mechanisms underlying DA-mediated function in health and disease are poorly understood at the level of systems biology despite an emerging picture of the relevant biomolecular pathways. Based upon decades of molecular studies, DA receptors can be grouped into D1-like and D2-like receptor families that produce opposing effects on the production of cyclic-AMP through activation or inhibition of adenylate cyclase (Neves et al., 2002; Stoof and Kebabian, 1981). The G-protein coupled D1 and D2 signaling pathways affect a host of functions, including regulation of metabolic enzymes, ion channels, and plasticity through gene transcription (Carlezon et al., 2005; Neves et al., 2002). Although the complexity of these cellular signaling pathways makes it difficult to define a precise mechanistic relationship between receptor binding and gross indices of tissue function, as measured by the group of techniques collectively called fMRI (BOLD signal, CBV, CBF, …), it is clear that D1 and D2 receptor families produce opposing effects at the top level of the G-protein coupled signaling cascade.

Use of selective dopaminergic agonists and antagonists can reveal the functional roles of D1 and D2 receptors *in vivo* using systemic administration and recording methods such as autoradiography to determine glucose utilization (*e.g.*, Trugman and James, 1993) or IRON fMRI to measure CBV (Mandeville, 2012). In rats, D1 agonism increases CBV in basal ganglia (Choi et al., 2006), whereas antagonism decreases CBV (Marota et al., 2000). Conversely, D2 agonists and antagonists produce effects on CBV that are opposite in sign to those produced by the respective D1 agents (Chen et al., 2005; Choi et al., 2006). These results clearly demonstrate that any understanding of DA-mediated function must consider the relative balance of D1-mediated excitation *versus* D2-mediated inhibition.

Viewing DA-mediated function in terms of opposing D1 and D2 contributions helps explain some subtle features of data in domains of dose and time and reconciles some pronounced differences observed across species and *versus* drug dosages. Amphetamine stimulation in the rat produces pronounced increases in CBV except at very small doses, where responses become slightly negative, an effect that was attributed to the high affinity of DA for a subset of D2-like receptors (Ren et al., 2009). In the

* Corresponding author. Fax: +1 617 726 7422.
  E-mail address: jbm@nmr.mgh.harvard.edu (J.B. Mandeville).

temporal domain, cocaine infusion produces a subtle decrease in CBV in rats prior to the dominant positive response (Chen et al., 2011; Marota et al., 2000; Schwarz et al., 2004), and segmentation of this temporal component produces a D2-like spatial map (Chen et al., 2011).

The most basic aspects of dopaminergic function appear to be similar across species except in the laboratory rat, one of the mainstays of scientific research. Glucose autoradiography reported cocaine-induced elevation of metabolism in rats (Porrino, 1993) but decreased metabolism in non-human primates (NHP) (Lyons et al., 1996) and mice (Zocchi et al., 2001). Similarly, IRON fMRI reported cocaine-induced elevation of CBV in rats (Chen et al., 2011; Marota et al., 2000; Schwarz et al., 2004) but decreased CBV in NHP (Mandeville et al., 2011) and wild-type mice (Perles-Barbacaru et al., 2011). Because the different fMRI responses in rats and NHP occur despite similar levels of evoked DA (Bradberry, 2000; Chen et al., 2010; Schwarz et al., 2004), we previously hypothesized that these different responses might be attributable to the ratio of D1 to D2 receptors (Mandeville et al., 2011), which is much higher in laboratory rats than in humans, NHP, or wild-type mice. Neuroadaptations in human cocaine-abusing populations, such as blunted dopamine release (Martinez et al., 2007) and down-regulated D2 receptor densities (Volkow et al., 1993), complicate a comparison with preclinical data, but the preponderance of evidence from a variety of neuroimaging techniques suggests that cocaine produces functional inhibition in human striatum in a manner similar to NHP results (Johnson et al., 1998; Kaufman et al., 1998; Kufahl et al., 2005; London et al., 1990; Wallace et al., 1996). However, the conundrum remains that cocaine infusion produces an opposite fMRI response in rats and NHP, but amphetamine stimulation increases CBV in both species at the doses that have been tested (Chen et al., 1999; Jenkins et al., 2004). This observation could be related to the different mechanisms of action between these drugs, or it might be that a single model can account for this difference based upon the different levels of DA induced by the two drugs.

This study describes a model of DA-induced function coupled to biochemistry through receptor occupancies using standard pharmacological principles. The goal was to develop an intuitive and extensible model that provides an integrative explanation of fMRI observations using dopaminergic drugs, while adhering to a mathematical approach that is testable using non-invasive neuroimaging. Predictions for fMRI signal are based upon a classical occupancy model driven by estimates in DA levels from the microdialysis literature. Because PET can detect changes in DA release through ^{11}C-raclopride displacement, albeit through mechanisms that are not fully understood (Ginovart, 2005), we acquired fMRI and PET data simultaneously in several sessions to evaluate relationships between these signals and the common unmeasured temporal function – evoked DA – that drives responses for both modalities. Note that D1-targeted PET ligands show little sensitivity to changes in DA levels, for reasons that may be related to ligand characteristics (Laruelle, 2000), so no D1-targeted PET studies were performed.

Model results are compared to prior literature and also to simultaneous PET/fMRI experiments in NHP using smaller doses of amphetamine than have been employed previously by fMRI studies using NHP (Jenkins et al., 2004). Although literature comparisons focus on preclinical results using the commonly employed IRON fMRI technique, the expectation is that the model calculations also will be applicable to future human studies based upon robust techniques like BOLD signal at very high field strengths, or the IRON method in standard clinical MRI scanners (Qiu et al., 2012). This model approach has been presented previously in preliminary form (Mandeville et al., 2012; Normandin et al., 2012a).

Methods

An fMRI model coupled to receptor occupancy

Pharmacological effects in biological systems often have been interpreted within the context of the classical receptor occupancy model (Clark, 1937), in which a response is a function of the fraction of receptors that are occupied. Furthermore, a classical occupancy model, or a "pure competition" model within the context of raclopride displacement studies (Ginovart, 2005; Laruelle, 2000), views receptors as static targets that are not dynamically regulated by processes like internalization within post-synaptic membranes. In developing a model for DA-induced fMRI signal, we adhere to the classical model and a simple linear coupling relationship between function and neuroreceptor occupancy. We postulate that a neurotransmitter evokes a functional response that can be expressed as a summation of changes in bound receptor densities, producing effects that can be either excitatory or inhibitory. Limitations of this viewpoint will be addressed in the Discussion section. In our notation, fMRI measurements are expressed as changes in CBV (ΔV) assuming the use of exogenous contrast agent, but the model is intended to apply to any measurements based upon changes in the blood supply using methods such as BOLD signal or CBF. Thus, a steady-state formulation of the model is

$$\Delta V(t) = \sum_i{}^{receptor\ types} N_i [B_i(t) - B_i(0)] \tag{1}$$

where changes in the concentration of bound receptors (B_i) are scaled by neurovascular coupling constants (N_i). In order to more directly associate the model with literature values and measurement methods, we separate the bound receptor densities into total receptor densities ($B_{max,i}$) and fractional occupancies ($\theta_i = B_i/B_{max,i}$),

$$\Delta V(t) = \sum_i N_i B_{max,i} [\theta_i(t) - \theta_i(0)]. \tag{2}$$

Changes in occupancy at a single receptor

Prior to considering a multi-receptor model for dopaminergic stimulation, we review a standard model for changes in occupancy at a single receptor derived from basic physiological principles. Using first-order kinetics and conventional terminology to describe a neurotransmitter communicating between free (F) and bound (B) compartments, the time-derivative of bound receptor is defined by the law of mass action (Michaelis et al., 2011):

$$\frac{dB(t)}{dt} = k_f B_{avail} F(t) - k_r B(t). \tag{3}$$

Binding exhibits saturation as the density of available receptors, $B_{avail}(t) = B_{max} - B(t)$, becomes small. Using the definition of the dissociation constant as the ratio of reverse to forward rate constants ($K_D = k_r/k_f$), and replacing the reverse rate constant with k_{OFF} for clarity, yields a standard first-order dynamic model for occupancy:

$$\frac{d\theta(t)}{dt} = k_{OFF}\left[(1-\theta(t))\frac{F(t)}{K_D} - \theta(t)\right]. \tag{4}$$

The model becomes more intuitive if we replace the absolute concentration of free neurotransmitter with the relative amount, as would be measured in the extracellular compartment by microdialysis or cyclic voltammetry. From the steady-state condition ($d\theta/dt(t<0) = 0$), the basal concentration of free neurotransmitter can be replaced with basal receptor occupancy and the dissociation constant for the neurotransmitter at the target receptor (K_D), yielding a differential equation for receptor occupancy that depends only upon basal occupancy and the offset (or dissociation) rate constant, in addition to the flux of neurotransmitter that drives the system:

$$f(t) \equiv \frac{F(t)}{F(0)}, \quad F(t) = F(0), \quad f(t) = K_D\frac{\theta(0)}{1-\theta(0)}f(t) \tag{5}$$

$$\frac{d\theta(t)}{dt} = k_{OFF}\left[(1-\theta(t))\frac{\theta(0)}{1-\theta(0)}f(t)-\theta(t)\right]. \tag{6}$$

The first term inside the square brackets contains the relative level of synaptic neurotransmitter concentration (f) that drives changes in occupancy, and the second term is the "resistance" due to finite head-room (i.e., θ cannot exceed 1, which corresponds to all receptors being bound).

A two-receptor model for dopaminergic stimulation

Although a general model like Eq. (1) is extensible, a fundamental challenge for all biological models is to simplify the framework to mini-mize unknowns and still capture enough complexity to describe the main features of data. Toward this goal, we compose a model consisting of only two receptor sub-types: D1-like receptors producing activation, and D2-like receptors producing inhibition. Fig. 1 illustrates the two-receptor model, which is defined by these equations:

$$\Delta V(t) = N_1 B_{max,1}\int_0^t \frac{d\theta_1(t')}{dt}dt' + N_2 B_{max,2}\int_0^t \frac{d\theta_2(t')}{dt}dt'$$

$$\frac{d\theta_2(t)}{dt} = k_{OFF,2}\left[(1-\theta_2(t))\frac{\theta_2(0)}{1-\theta_2(0)}f(t)-\theta_2(t)\right] \tag{7}$$

$$\frac{d\theta_1(t)}{dt} = k_{OFF,1}\left[(1-\theta_1(t))\frac{\theta_1(0)}{1-\theta_1(0)}f(t)-\theta_1(t)\right].$$

A slightly altered form of Eq. (7) emphasizes that the overall shape and sign of the modeled fMRI response depends upon ratios of recep-tor densities and coupling constants, as well as the quantities within the derivatives of occupancy.

$$\Delta V(t) = |N_2|B_{max,2}\left\{\frac{N_1}{|N_2|}\frac{B_{max,1}}{B_{max,2}}\int_0^t \frac{d\theta_1(t')}{dt}dt' - \int_0^t \frac{d\theta_2(t')}{dt}dt'\right\}. \tag{8}$$

Eq. (8) can be solved by iterative numerical integration subject to the initial conditions

$$\theta_1(0) = \frac{K_{D,2}}{K_{D,1}}\frac{\theta_2(0)}{1-\theta_2(0)}, \quad f(0) = 1. \tag{9}$$

Literature inputs to the model

Eqs. (7) and (8) have six fixed parameters and one temporal quan-tity describing DA efflux. Unless otherwise noted, values used for the fixed constants in our model calculations are those shown in Table 1, which are estimates from the literature.

Receptor densities (B_{max}) have been measured in rats and NHP by autoradiography, and PET also can estimate densities *in vivo* through binding potentials. Although there are variations in receptor densities re-gionally and across studies, the overall ratio of D1 to D2 receptors is slightly larger than unity in the basal ganglia of wild-type mice (Thompson et al., 2010), NHP (Madras et al., 1988; Weed et al., 1998),
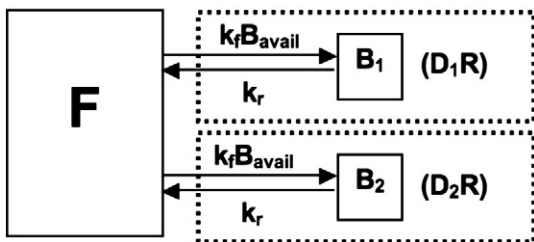

Fig. 1. A first-order two-receptor model for stimulation of D1 and D2 receptors by free dopamine (F).

Table 1
Model input values.

Quantity	Value
$\frac{B_{max,1}}{B_{max,2}}$	1.3 for NHP; 2.8 for rat
$\theta_2(0)$	0.25
$\frac{N_1}{N_2}$	1
$|N_2|B_{max,2}$	0.5% CBV per % DA occ
$\frac{K_{D,1}}{K_{D,2}}$	4
$k_{Off,1}, k_{Off,2}$	0.5 and 1 min^{-1}

and humans (Hall et al., 1994; Piggott et al., 1999). However, docile mice possess a high D1 to D2 receptor ratio in comparison with an ag-gressive strain (Couppis et al., 2008), suggesting that selective breeding for passivity can alter this ratio in laboratory rodents. In fact, laboratory rats possess a D1 to D2 receptor ratio in striatum of nearly 3 (Hyttel and Arnt, 1987; Schoffelmeer et al., 1994; Seeman, 1987). Weed et al. (1998) provided particularly good data on this subject by employing multiple concentrations of multiple ligands to measure D1 and D2 recep-tor densities in both rats and NHP; they concluded that macaque stria-tum (D1/D2 ratio = 1.2) does not display the relative overabundance of D1 receptors found in rat striatum (D1/D2 ratio = 2.6). A recent re-view of DA receptor densities across species found a markedly higher D1/D2 ratio in rats relative to human/NHP using either intact brain sec-tions or washed membranes (Cumming, 2011). The D1/D2 ratios shown in Table 1 are consistent with these data.

Basal D2 occupancy has been measured in human studies using DA depletion, with an average value of about 20% in normal control subjects across five such reports (Abi-Dargham et al., 2000; Laruelle et al., 1997a; Martinez et al., 2009; Verhoeff et al., 2001, 2002). Some-what larger D2 occupancy values have been reported in anesthetized NHP (Delforge et al., 2001; Ginovart et al., 1997; Laruelle et al., 1997b) using methodologies that were similar, but not identical, to the human studies.

In principle, neurovascular coupling constants can be measured in PET/MR experiments using selective agonists or antagonists to estimate the relationship between changes in occupancy and fMRI signal; in fact, we recently demonstrated a linear coupling between D2 receptor occu-pancy and the fMRI response in NHP basal ganglia due to progressive blocking of DA agonism at D2 by raclopride (Sander et al., 2012). Based upon this study and an assumption for D2 basal occupancy, the overall scale of model calculations was set by the measured function–occupancy relationship for whole putamen in NHP, $|N_2|B_{max,2} \approx 0.5\%$ CBV per % DA occupancy. Lacking any data on D1-mediated function *versus* occupancy, we assume here that the D1 and D2 coupling con-stants are similar in magnitude but opposite in sign.

The offset rate constants also are unknown, but these only have a modest effect on the shape of the model response as long as they are not too dissimilar and are fast compared to the time scale of DA release, which evolves over many minutes. Although ratios of offset and onset constants are defined by dissociation constants (K_D), the absolute values of these individual parameters typically are not measured in *in vitro* binding assays. Dopamine offset rates have been estimated to be within the range 0.3 to 6 min^{-1} (Logan et al., 1991). In model simula-tions, we used 0.5 min^{-1} and 1 min^{-1} for the k_{OFF} values of DA binding to D1 and D2 receptors, respectively. The choice of these two parame-ters can affect the initial onset response of fMRI signal.

One of the most critical parameters in the model is the affinity ratio of DA for D1 and D2 receptors, expressed as the K_D ratio in Table 1. A re-cent binding assay using both human and rat receptors found that DA has a much higher affinity for D2 receptors relative to D1 receptors (Marcellino et al., 2011), in agreement with one older study that found a higher affinity for D2 receptors but concluded that both types of receptors exhibited similar functional affinities, based upon adenyl-ate cyclase activity (Schoffelmeer et al., 1994). Conversely, two reports found similar D1 and D2 binding affinities for DA (Madras et al., 1988; Sokoloff et al., 1992), although the latter study also reported high

affinities for D3 and D5 relative to either D1 or D2 receptors. We assumed an affinity ratio of 4 in favor of the D2-family of receptors relative to the D1 family, based upon inhibition constants for human receptors (Marcellino et al., 2011). However, this affinity ratio is not well constrained by available data.

In addition to the fixed quantities in Table 1, the model requires knowledge of the magnitude and timing of DA release. Simulations are presented for conditions corresponding to IV infusion of 0.5 mg/kg cocaine and IV infusion of 0.6 or 1 mg/kg amphetamine. To model previous fMRI results for cocaine administration in awake NHP (Mandeville et al., 2011), we relied upon the DA microdialysis measurements in awake NHP using the same cocaine dose and a temporal resolution of just 2 min (Bradberry, 2000). DA microdialysis in rats using this cocaine dose shows a similar magnitude response, potentially with a slightly extended release profile (Chen et al., 2010; Frank et al., 2008) as might be expected due to an extended drug blood half life in the anesthetized condition. Because amphetamine stimulates DA release, much higher levels of evoked DA can be achieved. For amphetamine doses up to 1 mg/kg in the rat, a linear fit to microdialysis data *versus* dose in units of mg/kg yields %DA = 2270 ∗ dose (Ren et al., 2009). Pooling NHP data across studies (Endres et al., 1997; Kirkland Henry et al., 2009; Laruelle et al., 1997b), the linear fit is %DA = 1976 ∗ dose. For these calculations, we used amphetamine-induced peak DA magnitudes of 1000% at 0.6 mg/kg and 2000% at 1 mg/kg, with a time-to-peak equal to 20 min (Kirkland Henry et al., 2009; Ren et al., 2009).

Amphetamine-induced fMRI response in NHP

Two simultaneous PET/fMRI experiments were performed in one rhesus macaque monkey using doses of 0.6 and 1.0 mg/kg amphetamine, and fMRI results at the higher dose were replicated in a second monkey in the absence of PET. In each study, anesthesia was induced with injected agents (20 mg/kg ketamine and 0.4 mg/kg diazepam) and maintained by isoflurane (1% to 1.5%) in oxygen through an intubation tube without ventilation. Venous lines were placed in saphenous veins of the lower leg for injections of MRI contrast agent (Feraheme, 10 mg/kg), PET ligand (^{11}C-raclopride), and amphetamine. Physiological parameters (blood pressure, pulse rate, oxygen saturation, end-tidal CO_2, and respiratory rate) were monitored throughout experiments. Procedures complied with the regulations of the Subcommittee on Research Animal Care at Massachusetts General Hospital.

Functional MRI employed the IRON method (Mandeville, 2012) in conjunction with single-shot EPI that was accelerated by a factor of two in the phase-encode direction in order to provide an isotropic spatial resolution of 1.3 mm with an echo time of 23 ms. Whole brain volumes were collected every 3 s. fMRI analyses followed previously described procedures (Mandeville et al., 2011) for registration to a brain atlas (Saleem and Logothetis, 2006) and MRI template (McLaren et al., 2009) and for time-series analysis using the general linear model.

PET raclopride displacement data were acquired to provide an independent correlate of dopamine release in order to further evaluate assumptions employed in the fMRI model. Simultaneous PET/fMRI imaging data were acquired in a 3 T MRI scanner (MAGNETOM Trio, Tim System, Siemens AG, Healthcare Sector, Erlangen, Germany) with an MRI-compatible PET insert (BrainPET, Siemens AG, Healthcare Sector, Erlangen Germany; Schmand et al., 2007). PET list-mode data were sorted in the line-of-response space and reconstructed with the ordinary Poisson-ordered subsets expectation maximization algorithm. Data were binned into 1-minute intervals except during the first 5 min of uptake, where bins were reduced to 30 s.

Raclopride was synthesized using standard techniques (Farde et al., 1985) with minor modifications. In one study, administration of 0.6 mg/kg amphetamine occurred 30 min after a bolus injection of 3.8 mCi ^{11}C-raclopride. In the second study, amphetamine administration occurred at the same time point relative to the bolus infusion, but PET ligand was injected as a bolus plus continuous infusion paradigm

used a "K_{bol}" of 50 min, a value derived from prior bolus data without challenge (Carson et al., 1993); the injected activity in the bolus of the second experiment was 4.5 mCi.

PET analysis used a general linear model implementation (http://www.nitrc.org/projects/jip) of the simplified reference tissue model (Lammertsma and Hume, 1996) with two parameters (Ichise et al., 2003) and a time-varying binding term (Alpert et al., 2003; Normandin et al., 2012b) to determine a temporal quantity, $k_{2a}(t)$, that can be related to a dynamic binding potential (DBP_{ND}) relative to non-displaceable binding that is analogous to an equilibrium binding potential. Using the definition for k_{2a} (Lammertsma and Hume, 1996), we defined a dynamic quantity

$$DBP_{ND}(t) \equiv \frac{k_2}{k_{2a}(t)} - 1. \tag{10}$$

The temporal form of $k_{2a}(t)$ was determined by minimizing the chi-squared per degree of freedom for SRTM fits by varying the parameter τ in predefined functional forms that were either gamma-variate ($^t/_\tau e^{-t/_\tau}$) or sigmoidal ($t/\tau/\sqrt{1 + (t/\tau)^2}$) functions.

Within the context of a "pure competition" or "classical occupancy" model (Ginovart, 2005; Laruelle, 2000), relative changes in DA efflux can be determined from raclopride displacement studies; accordingly, significant temporal or magnitude deviations from the microdialysis literature would suggest a violation of the classical occupancy model. As in Eq. (6), changes in raclopride occupancy using a tracer dose of ligand ($\theta_R \approx 0$) can be written as

$$\frac{d\theta_R(t)}{dt} = k_{OFF,R} \left[(1 - \theta_{DA}(t)) \frac{\theta_R(0)}{1 - \theta_{DA}(0)} f(t) - \theta_R(t) \right] \tag{11}$$

and peak levels of DA release can be estimated by setting the derivative to zero to obtain

$$f^{max} = \frac{\theta_{DA}^{max}(1 - \theta_{DA}(0))}{\theta_{DA}(0)(1 - \theta_{DA}^{max})}. \tag{12}$$

Maximum changes in DA levels can be related to relative changes in DBP_{ND} (Eq. (10)) using

$$DBP_{ND}^{min} = \frac{B_{max}(1 - \theta_{DA}^{max})}{K_D} \Rightarrow \frac{DBP_{ND}(0)}{DBP_{ND}^{min}} = \frac{(1 - \theta(0))}{(1 - \theta_{DA}^{max})},$$

$$\text{or} \quad f^{max} = 1 + \frac{1}{\theta(0)} \left(\frac{DBP_{ND}(0)}{DBP_{ND}^{min}} - 1 \right). \tag{13}$$

When estimating evoked DA from Eq. (13), we employed the D2 basal occupancy value from Table 1. Hence, PET measurements within a pure competition model can provide an estimate of the relative magnitude of evoked DA (f) that is assumed in the fMRI model.

Because SRTM does not separate the free and non-specifically bound compartment from specific binding (Lammertsma and Hume, 1996), we performed forward-model simulations using separate specific and non-specific compartments to estimate the degree of error associated with using DBP_{ND} as an index of specific binding. Simulations used literature values for rate constants and adjusted the simulated time–activity curves to approximately match data prior to amphetamine injection. Simulations were analyzed using the DBP_{ND} metric, and these were compared to the known dynamic quantity $B_{avail}(t)/K_D$ from the simulations. Additionally, simulations estimated the magnitude of change in time–activity curves due to amphetamine-induced changes in blood flow, which alter delivery and washout rates. Such simulations have been reported previously by others for raclopride (Alpert et al., 2003; Normandin and Morris, 2008; Pappata et al., 2002) based upon estimated ranges for changes in CBF. We estimated changes in CBF directly from measured changes in CBV assuming a power–law relationship between these quantities (Grubb et al., 1973); in turn, changes in CBF

were converted to changes in the delivery (K1) and washout (k2) rates using the Renkin–Crone equation.

Results

To investigate model accuracy relative to data published previously or acquired in this study, we first generate simulations employing the model defined by the parameters in Table 1 and by the DA efflux curves described in the Methods. Figs. 2, 3, and 4 conform to this fixed model. We then evaluate the sensitivity of the model to changes in individual parameters across ranges defined by our estimates of literature variance (Fig. 5), and we also investigate covariance between parameters that can lead to similar model results by simultaneously varying two parameters (Fig. 6). Finally, we present PET data that were acquired simultaneously with fMRI responses in order to assess shortcomings of the model and the potential for combining the multimodal information.

Model description of prior pre-clinical fMRI data

Simulations in Fig. 2 employ the parameter set shown in Table 1, together with a function for DA release defined by the red curve in Fig. 2a (Bradberry, 2000), in order to provide model predictions corresponding to a cocaine dose of about 0.5 mg/kg in the laboratory rat *versus* NHP. Note that the basal occupancy by DA at D2 receptors is about 3-fold higher than the D1 occupancy in the model as a consequence of the presumed ratio of affinities (Eq. (9)). Accordingly, the higher affinity of DA for D2 receptors drives a more rapid increase in D2 occupancy relative to D1 occupancy following the onset of DA release. Even for such a strong increase in synaptic DA (400%), ceiling effects due to receptor saturation are not pronounced, so the total increase in D2 occupancy near the peak of the DA surge is about two-fold greater than the net increase in D1 occupancy. Hence, the functional response (Fig. 2b) will be negative in Eq. (8) as long as the receptor densities or neurovascular couplings are not heavily weighted in favor of the excitatory D1 family. For NHP, which has similar D1 and D2 densities, the negative model response matches fMRI data in this species (Mandeville et al., 2011). In the rat, the overall sign of the model response is reversed after a brief negative dip by changing only the D1/D2 receptor ratio in the model; this response in the rat matches fMRI data reported by our group and others (Chen et al., 2011; Marota et al., 2000; Schwarz et al., 2004). Moreover, recently reported mouse fMRI data show a cocaine-induced reduction in CBV in basal ganglia similar to the NHP (Perles-Barbacaru et al., 2011), as predicted by the model due to the similar density of D1 and D2 receptors in the mouse. The temporal response in the mouse study was delayed and protracted relative to the model results

of Fig. 2, which presumably is a consequence of the intraperitoneal route of drug administration.

Several previous studies have provided empirical evidence that the temporal evolutions of fMRI signal and DA are very similar under some circumstances in both rat and NHP. To address this issue under specific circumstances, Fig. 3a shows simulation results using standard parameters (Table 1) and the measured DA profile from Chen et al. (1999) to show that the fMRI model indeed matches the DA release profile using high doses of amphetamine in the rat. In this case, the high D1 to D2 receptor ratio in rat striatum causes D1-mediated stimulation to dominate D2-mediated inhibition, so that fMRI signal becomes a virtual surrogate for DA release in the temporal domain. In NHP and humans, striatum contains similar levels of D1 and D2 receptors, and the model predicts that the evolution of fMRI signal will reflect DA release relatively well only at low levels of evoked DA, where D2 effects should dominate due to the higher affinity of DA for D2. Fig. 3b employs the DA release profile in NHP for cocaine, using half the magnitude reported for a dose of 0.5 mg/kg (Bradberry, 2000), for comparison with the fMRI model using this DA function. We previously noted that empirical fMRI responses using 0.25 or 0.5 mg/kg cocaine in NHP agreed quite well with the DA profile reported by Bradberry (Mandeville et al., 2011), and the model calculations of Fig. 3b match this empirical conclusion. Note that the sign of the fMRI response in NHP has been reversed in Fig. 3b for comparison with the DA curve.

fMRI response to amphetamine in NHP

The high affinity of DA for D2-like receptors determines the sign and magnitude of model responses in NHP at levels of evoked DA up to a few hundred percent, as produced by cocaine administration, but we can stress the model by further increasing evoked DA to reveal effects of D2 receptor saturation in fMRI signal. Amphetamine provides a means to do this.

Fig. 4 includes model simulations with data from whole putamen acquired in this study. Data were corrected by removing uninteresting regressors (e.g., polynomial baseline drift, motion correction parameters) and by binning the 3-second acquisitions into 30-second intervals for presentation. Unlike a previous report of a positive CBV response in basal ganglia of NHP due to 2.5 mg/kg of amphetamine (Jenkins et al., 2004), the measured response using an amphetamine dose of 0.6 mg/kg clearly was negative in NHP striatum (Fig. 4a). At a dose of 1 mg/kg amphetamine, a biphasic shape described the CBV data best, with a rapid and pronounced initial decrease followed by an overshoot that resolved slowly toward baseline.

Simulations provided a good description of these data. In analysis, simulations provided model shapes (red curves) that were used as
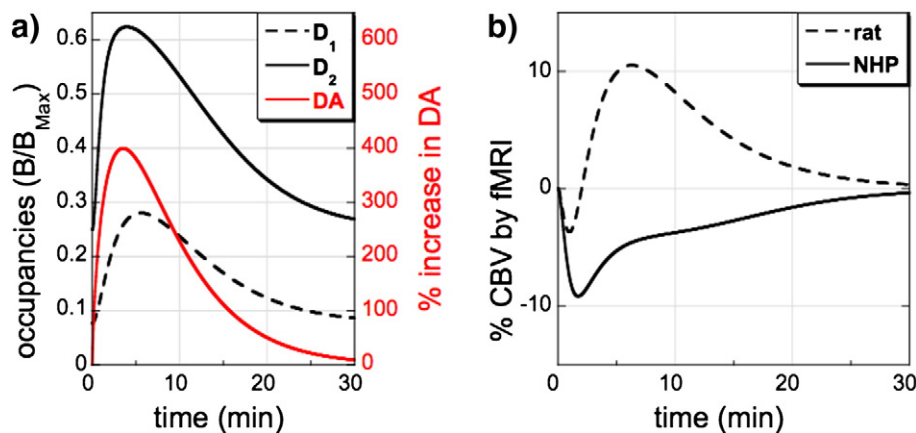

Fig. 2. Model inputs and results corresponding to a cocaine dose of about 0.5 mg/kg in rat and NHP. a) 400% increase in DA produces a larger relative change in D2 occupancy relative to D1 occupancy by virtue of dopamine's higher affinity for D2 receptors. b) fMRI responses initially decrease in both species, but the high ratio of D1 to D2 receptors reverses the overall sign of the cocaine-induced response in the rat.
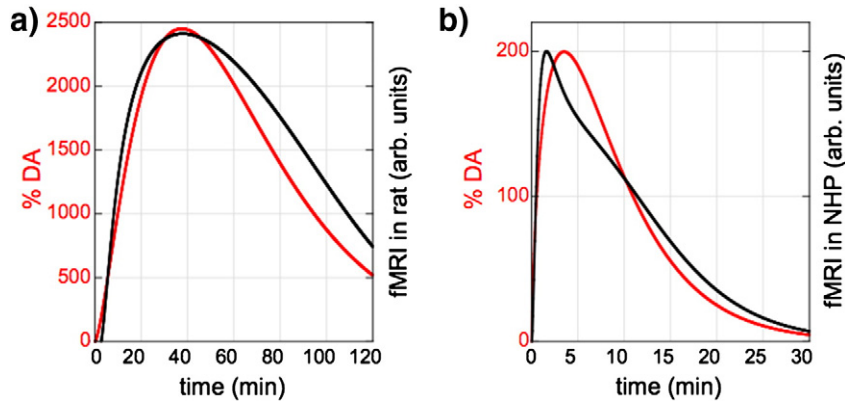
Fig. 3. Scenarios in which the predicted fMRI response closely reflects the temporal evolution of evoked dopamine (DA). a) High levels of evoked DA in the rat cause D1 effects to dominate, so that fMRI signal matches DA in time, in agreement with empirical data using amphetamine infusion in rats (Chen et al., 1999). b) Low levels of evoked DA, as would be expected using about 0.25 mg/kg cocaine, cause D2 effects to dominate in NHP; note that the fMRI sign has been reversed in NHP for comparison with DA.

regressors for the general linear model, which applied overall scale factors to each data set. The functional map in the figure shows the magnitude of the analysis regressor using a color scale with a CBV threshold of 5% for all voxels that passed a statistical threshold of $p < 10^{-2}$ after correction for multiple comparisons. At the low dose (0.6 mg/kg), the model predicts a decrease in CBV in agreement with data. For the level of DA associated with a dose of 1 mg/kg, the model predicts a rapid initial drop in CBV followed by a positive overshoot that resolves back to baseline much more rapidly than the DA input function. At times later than 50 min, the model response of CBV falls below zero, but it would difficult to experimentally distinguish this effect from baseline drift.

Amphetamine produced large and prolonged increases in blood pressure as measured by an arm cuff with virtually no change in other physiological parameters like respiratory rate or end-tidal CO_2, so we cannot exclude the possibility that a portion of the CBV decrease resulted from vasoconstriction as an autoregulatory response. In rats, relatively large changes in blood pressure across the autoregulatory range produce only very small changes in CBV using models of

hypotension (Zaharchuk et al., 1999) or injected drug (Gozzi et al., 2007; Liu et al., 2007). At the 0.6 mg/kg dose in this study, a decrease of about 5% CBV was observed in most regions outside basal ganglia, and this could be due to either autoregulation or the specific effects of amphetamine. At all doses, CBV reductions were about 2.5 times larger within basal ganglia than in other areas, demonstrating that focal CBV decreases in basal ganglia exceeded any global effects.

Parameter sensitivity and covariance

Fig. 5 demonstrates the sensitivity of individual parameter selections using the DA driving function from Fig. 2a, corresponding to a cocaine dose of about 0.5 mg/kg. In each panel, one parameter is varied while all other parameters are fixed according to Table 1. The parameter that perhaps is most constrained by the literature is the D1/D2 receptor ratio (Fig. 4a), which is 1.2 to 1.4 in two studies using autoradiography in NHP (Madras et al., 1988; Weed et al., 1998) and about unity in human postmortem caudate and putamen (Hall et al., 1994; Piggott et al., 1999). *Given the similar densities of D1 and D2 receptors, the model*
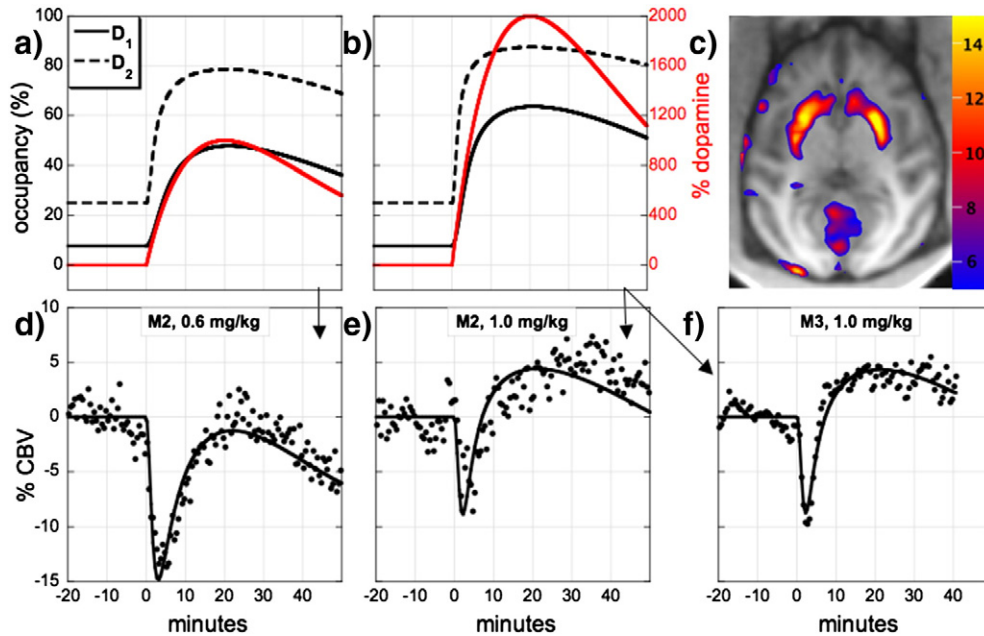
Fig. 4. Simulations were performed for two doses of amphetamine (0.6 and 1 mg/kg) that were assumed to increase synaptic dopamine 10-fold and 20-fold (blue curves), respectively. Simulation results for fMRI signal were employed as GLM analysis regressors (red curves) to describe data from whole putamen (black points) with a single scaling factor after correction for baseline drift using a quadratic polynomial. The functional map from one session (M3, 1 mg/kg) shows voxels that were significantly correlated with the regressor and exhibited maximal changes in CBV greater than 5%.
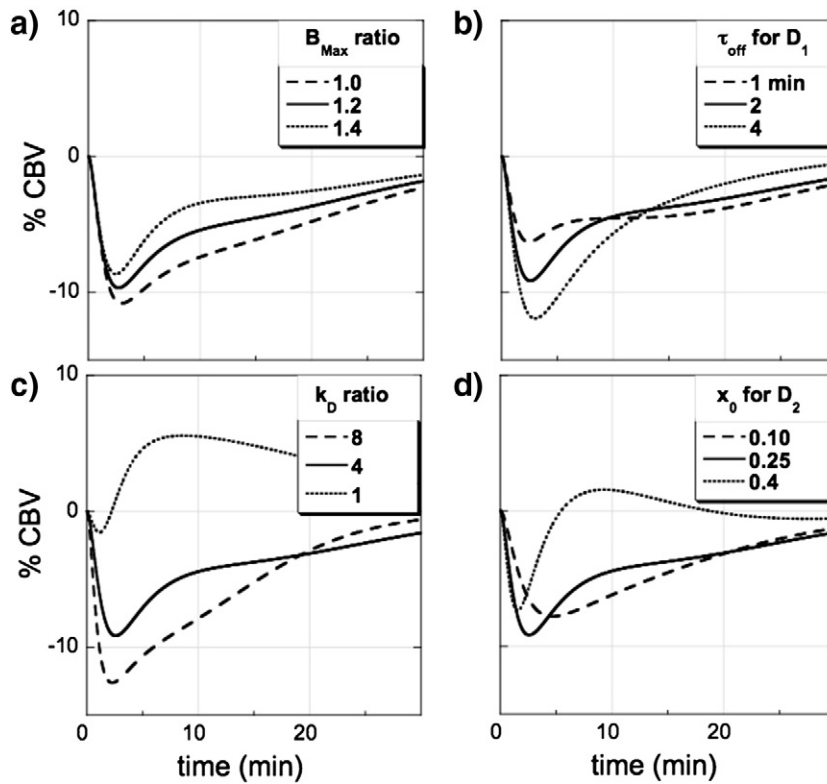
Fig. 5. Simulations show the effect of varying individual parameters in Table 1, assuming the dopamine release function in Fig. 2a. Parameter choices are discussed in the text. Note that the fMRI model cannot reproduce data in NHP for cocaine infusion (Mandeville et al., 2011) or amphetamine administration (Fig. 4) unless dopamine affinity is strongly biased in favor of D2 relative to D1 receptors.
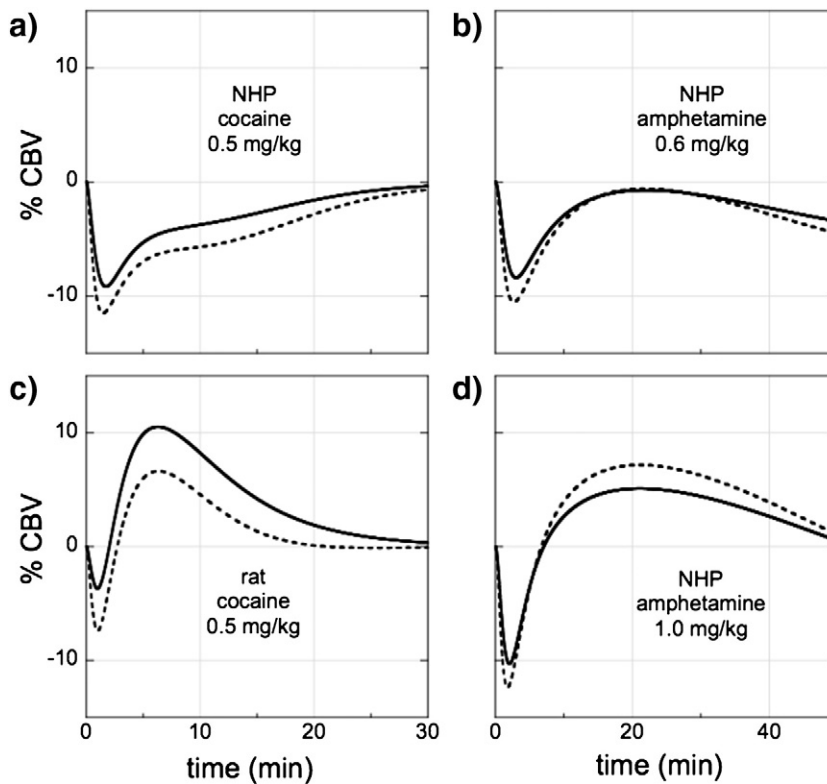
Fig. 6. Model calculations demonstrate the covariance between basal occupancy and the relative affinity of dopamine for D2 relative to D1 receptors, using the dopamine input functions of Figs. 2 and 3. Solid lines use the parameter set of Table 1, including a D2 basal occupancy of 25% and an affinity ratio of 4. Dashed lines use a D2 basal occupancy of 40% and an affinity ratio of 10.

cannot reproduce measured NHP or mouse fMRI data with any combination of parameters unless DA affinities are strongly biased toward D2 receptors (Fig. 5c). Conversely, variation of D2 basal occupancy (Fig. 5d) or the relative values of the offset time (1/k$_{off}$, Fig. 5b) can produce differences in shape, but do not fundamentally alter the inhibitory nature of the model response.

Although Fig. 5 shows variations in individual parameters, it does not address how simultaneous variation in multiple parameters might produce redundant solutions. In Fig. 6, we fix all parameters according to Table 1 and then simultaneously vary both D2 basal occupancy and the affinity of DA for D2 relative to D1. These two parameters together determine relative changes in D1 and D2 receptor occupancy by DA, and each is relatively difficult to accurately measure with existing methods, as evidenced by the wide dispersion of literature results. Solid lines use the parameter set of Table 1 for the calculations as previously described in the Methods and presented in Figs. 2–5. Dashed lines use an alternative combination of D2 basal occupancy (0.40 versus 0.25) and D2/D1 affinity (10 versus 4). A larger relative affinity of DA for D2 receptors can negate a higher basal D2 occupancy, which limits the excursion range of changes in D2 occupancy by defining the rate of receptor saturation. Hence, the model can produce almost redundant solutions by covarying D2 basal occupancy and affinity, so that one value is needed in order to fix the other.

PET correlates of DA release

In two studies, corresponding to the two panels of Fig. 4 labeled as monkey M2, we acquired PET data in conjunction with fMRI (Fig. 7). In each study, a single sigmoidal function fits the time–activity curve with a lower chi-squared per degree of freedom than any gamma-variate function. In other words, raclopride binding in basal ganglia after amphetamine infusion did not exhibit any measurable indications of a return to pre-amphetamine levels during the imaging sessions, in agreement with prior studies (Laruelle, 2000).

For the injected dose 0.6 mg/kg amphetamine (Fig. 7a), DBP$_{ND}$ (Eq. (10), thick red curve) was suppressed by a maximum of 65–70% in putamen, depending upon the size of the region of interest, at the end of data collection. This corresponds to about a 9-fold increase in DA, which is similar to peak levels from the microdialysis literature. However, the response was slow and protracted compared to the analysis of simulated data in Fig. 7a (thin red line) that incorporated the DA release profile of Fig. 4. The metric DBP$_{ND}$ from analysis of the simulations proved to be a reasonably accurate index of true receptor availability (dashed red line) in the simulations.

Similar results were obtained using the higher dose of 1 mg/kg (Fig. 7b). Raclopride binding in putamen was suppressed by a maximum value of 55–60% by the end of the scan, corresponding to an estimated 6-fold increase in DA, and the optimal sigmoidal time constant was 85 min. Again, these changes in raclopride binding were blunted and occurred much more slowly than suggested by classical-model simulations based upon the microdialysis literature.

To ensure that measured changes in time–activity curves were specific to binding, rather than delivery and washout, we performed forward-model simulations based upon measured amphetamine-induced changes in CBV. Maximum flow-induced reductions in delivery and washout rates were estimated to be less than 10% for the CBV changes shown in Fig. 4d, and effects on simulated time–activity curves were negligible. These results agree with previous reports (Alpert et al., 2003; Normandin and Morris, 2008) and emphasize that these PET responses to amphetamine can be interpreted in terms of neurochemistry with little sensitivity to hemodynamics.

Discussion

The goal of this report was to develop a simple and testable receptor-based model capable of producing a consistent description of the growing body of preclinical fMRI data using drugs of abuse and selective agonists and antagonists. The model produces compelling descriptions of literature data and also predicts a new observation—the functional response of NHP basal ganglia to amphetamine is inhibition at moderate doses and a biphasic response at higher doses. We discuss assumptions, limitations, and potential modifications of the model, as well as applications of the model for experimental design and analysis and for studies of neurovascular physiology and connectivity.

Neurovascular coupling assumptions and limitations

Many factors can drive fMRI signal, and so an unstated but obvious assumption underlying the model is that the effect of drug can be disentangled from other contributing factors. In addition to drug-induced perturbations of systemic physiology, significant sources of activation in human subjects or awake animals can be associated with cognitive or volitional motor processes that may not be directly driven by the infusion of drug. For instance, human BOLD studies of cocaine self-administration in cocaine-using subjects have identified frontal cortical activation that is associated with cues or subjective ratings of craving (Risinger et al., 2005; Wilson et al., 2004), and NHP models also report frontal activation associated with conditioned cocaine visual
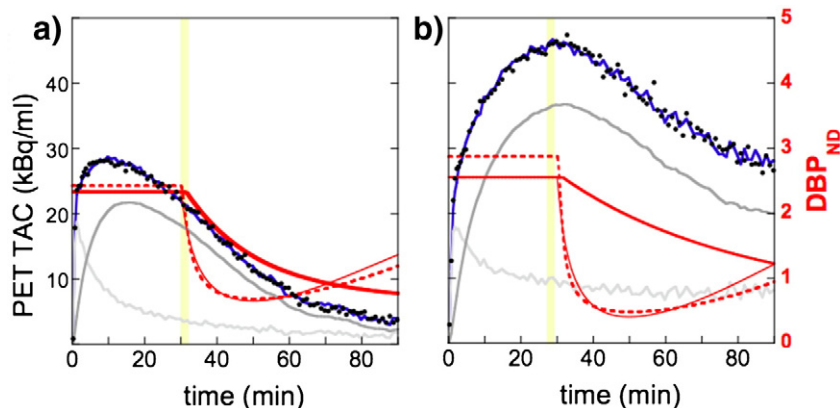
Fig. 7. PET data obtained following a bolus infusion of ^{11}C-raclopride with i.v. infusion of 0.6 mg/kg amphetamine (a), or by a bolus plus continuous infusion protocol with i.v. injection of 1 mg/kg amphetamine (b). The yellow bar is the injection interval at 30 min. PET time–activity curves (black), together with SRTM fits (blue) decomposed into curves weighted by delivery of ligand (R$_1$ ∗ C$_R$, light gray) and specific binding (C$_T^{Fit}$ − R$_1$ ∗ C$_R$, dark gray), are shown together with a time-dependent unitless binding term (DBP$_{ND}$, Eq. (10), thick red curves, right axis). Simulation results are overlaid for comparison with DBP$_{ND}$: thin red curves represent DBP$_{ND}$ analyses of a forward-model simulation base upon a pure competition between raclopride and dopamine, with DA curves identical to the model simulations in Fig. 4, and dashed red curves illustrate modeling errors by showing the true value of B$_{avail}$/K$_D$ within the simulations.

stimuli in the absence of drug delivery (Nelissen et al., 2012). Many such effects can be tested through temporal analyses and control experiments.

Neuroreceptor stimulation generally can be expected to produce non-local activation or inhibition through axonal pathways, so that the neural response in any tissue volume might reflect an unknown admixture with non-local effects. This potential confound applies to all correlations between fMRI signal and local measurements based upon neurochemistry, electrophysiology, or other aspects of tissue function. The rich dopaminergic innervation of basal ganglia in comparison with extrastriatal regions may reduce influences of non-local effects upon functional response to dopaminergic drugs within basal ganglia, particularly when responses are assessed as large regions of interest.

The model described here is predicated upon the assumption that changes in neuroreceptor occupancy drive the fMRI response. This association suggests a predominant role of post-synaptic processes in evoking fMRI signals. If the model is tied to measurable changes in occupancy using PET, then measurements cannot distinguish between presynaptic and postsynaptic receptors. Presynaptic autoreceptors function primarily as a negative feedback mechanism to regulate neurotransmitter release, which is explicitly incorporated into the model as the driving function for changes in postsynaptic occupancy. However, neurotransmitter release and reuptake presumably require metabolic support that is not incorporated into the model in the current form.

The fact that amphetamine stimulation produces functional inhibition at a dose as large as 0.6 mg/kg, which corresponds to a very high level of DA release, suggests that neurotransmitter release is not the dominant influence on the fMRI response to dopaminergic drugs. This observation is consistent with estimates that post-synaptic signaling dominates the energy expenditures associated with neural communication (Attwell and Laughlin, 2001). Nevertheless, presynaptic processes may contribute to DA-induced fMRI signal in a way that is difficult to distinguish from post-synaptic D1-mediated activation. In fact, the model predicts that a measurable initial decrease in CBV should persist in the NHP even at higher doses of amphetamine than employed in this study, but doses like 2.5 mg/kg did not show evidence of a sizable initial dip using modest temporal resolution (Jenkins et al., 2004). Presynaptic contributions from DA release could falsify this model prediction, but other factors discussed below, like receptor internalization, could preferentially blunt the D2 response more than the D1 response at high levels of evoked DA.

Calibrating and refining the model by PET/fMRI

An important feature of this fMRI model is that most of the variables in the model can be measured in principle by PET and fMRI experiments. For instance, scaling factors for the D1 and D2 arms of the model (e.g., $N_2B_{max,2}$), as well as the degree of linearity between occupancy and function, in principle can be determined using graded doses of selective agonists and antagonists. Preliminary data by our group support the notion of a roughly linear coupling between fMRI signal and DA occupancy at D2 receptors based upon variable doses of a D2 antagonist (Sander et al., 2012). Similarly, tracer doses of PET radioligands can measure relative regional receptor densities using ratios of D1 or D2 binding potentials to eliminate uncertainty in dissociation constants.

Basal receptor occupancy is an important variable in the model that is not routinely measurable by PET, although DA depletion has been used in humans and NHP to estimate basal D1 and D2 occupancies. As an alternative strategy to DA depletion, it may be possible to obtain information about basal occupancy from simultaneous PET/fMRI experiments using targeted drugs. When employing non-tracer doses of exogenous agonist or antagonist, the induced fMRI signal always will be a function of the basal occupancy of endogenous neurotransmitter at the target receptor; for instance, the maximal fMRI response using a targeted antagonist will depend upon the maximum displacement of neurotransmitter, which is set by basal occupancy. Of course, careful

studies of the mechanisms underlying specific fMRI responses using targeted ligands will be required to demonstrate that responses are specific to the neuroreceptor under investigation.

Another important parameter of the model, the affinity ratio of DA for D1 relative to D2 receptors, is a function purely of the D1 and D2 basal occupancies (Eq. (9)), so that measurements of basal occupancies specify the affinity ratio. As reviewed in the Methods, the average value of D2 occupancies across studies is about 20%. If DA has a lower affinity for D1 receptors, then basal D1 occupancy should be lower than the value reported for D2 receptors. In fact, studies to date in humans and preclinical models have not shown a measurable effect of DA depletion on D1 binding potentials, suggesting that D1 basal occupancy is very low indeed (Chou et al., 1999; Guo et al., 2003; Verhoeff et al., 2002). However, alternative mechanisms that invoke ligand-specific characteristics, such as high lipophilicity and environment-sensitive changes in affinity due to ligand trapping inside cells (Laruelle, 2000), also potentially could attribute to the relative insensitivity of changes in D1 binding potential following DA depletion.

Applications of the model

Explicit models of fMRI signal based upon measurable aspects of neurochemistry can be used to test hypotheses about neurovascular coupling, to interpret the relationship between neuroadaptations and inferences of function based upon the blood supply, and to guide the design and analysis of basic science and clinical investigations. For instance, to aid experimental design in a study of progressive drug exposure, model calculations can suggest a test dose of drug that is optimally sensitive to shifts in the fMRI response magnitude. The response magnitude initially should increase with increasing levels of evoked DA, and then the magnitude and integral of the response should decrease and eventually change sign at higher levels of DA, as D1-mediation activation begins to counter D2-mediated inhibition. Thus, the sensitivity of fMRI signal changes to neuroadaptations should be expected to vary as a function of drug dose.

For data analyses, model calculations can provide regressors for temporal analyses, as illustrated in Fig. 4. This strategy is arguably more important in a low contrast-to-noise regime using functional imaging methods like BOLD signal or arterial spin labeling, where the shape of the response is less readily apparent from the data. Optimal ways to employ model predictors in data analyses will require further exploration. A single fMRI regressor, as used in Fig. 4, is statistically more efficient than using separate D1 and D2 regressors, but the latter method provides more information in principle by segmenting the response into maps mediated by D1 and D2 binding and connectivity. Temporal regressors based upon predictions of D1 and D2 occupancy provide one strategy for separating the D1 and D2 components, but these regressors are only subtly different, so covariance will degrade statistical power in such an analysis. Linear combinations of occupancy predictors that separate fMRI signals into fast and slow components might offer a more statistically robust separation of temporal components. Such strategies have been employed previously in fMRI analyses (Chen et al., 2011; Liu et al., 2007), although regressors were not related to predictions of occupancies.

Finally, analyses in principle could opt to replace fMRI signal with DA release as an outcome measure, although additional work will be needed to determine errors using this approach. Because PET and fMRI signals both are sensitive to the same function of DA release ("f" in Eqs. (7) and (11)) but with different sources of error, combined measurements should offer a better estimation of neurotransmitter release. In this study, very high levels of evoked DA provided a means to test the model, but most pharmacological challenges with neuroscience or clinical relevance evoke much lower levels of DA, which may provide a number of advantages in terms of interpretability. At lower DA levels, fMRI signal is expected to provide a reasonably close temporal description of DA efflux (Fig. 3b). Interpretation of PET displacement studies

also may be simplified at lower DA levels if receptor endocytosis, as discussed below, is less pronounced.

Breakdown of the classical occupancy model: implications for fMRI model

It is likely that some refinements of the model will be required in order to incorporate aspects of *in vivo* neurochemical physiology that are subject to ongoing investigation: potential confounds include multiple affinity states and receptor internalization. Experimental PET observations implicating these mechanisms during DA release include an apparent "ceiling effect" on changes in binding potential and an extended period of raclopride displacement that persists much longer than microdialysis measurements (Laruelle, 2000). In our data (Fig. 7), changes in raclopride displacement occurred more slowly than the microdialysis literature would predict; this difference could represent a combination of temporal persistence and a ceiling effect.

If multiple affinity states exist *in vivo*, a controversial topic due to highly disparate results (Cumming, 2011; Skinbjerg et al., 2012), then low-affinity states presumably would be available to the antagonist raclopride but not to agonists like DA (Narendran et al., 2005). Similarly, a static pool of unbound receptors internalized within cellular membranes would be unavailable to DA but available to raclopride with a reduced affinity (Guo et al., 2010). Either of these mechanisms would limit apparent raclopride displacement by DA, such that estimates of DA release based upon a classical occupancy model (Eq. (13)) would underestimate actual changes. Incorporation of either of these effects into the fMRI model would be equivalent to increasing the basal occupancies to account for a higher fraction of unavailable receptors in the basal condition.

However, static effects alone cannot reconcile our PET data with assumptions from the microdialysis literature or with fMRI responses that are interpreted within our model. From the fMRI data, competition between D1 and D2 binding at high DA levels prevents a simple model-free interpretation, but a reasonable interpretation of Fig. 4d is that DA levels are no longer increasing at times later than 20 min. For each of the studies, simulations based upon the microdialysis literature produced a good agreement with fMRI data, although signal changes in the tail of response are difficult to separate from baseline drift.

The simplest explanation that can unite these observations is DA-induced receptor internalization, as reviewed by others in the context of PET observations (Ginovart, 2005; Laruelle, 2000). Compared to the temporal response of DA efflux, receptor endocytosis should prolong raclopride binding but abbreviate the fMRI response by dynamically down-regulating target receptors. Thus, receptor internalization is expected to cause a temporal divergence of the PET and fMRI signals that should become more apparent at high levels of DA or injected agonist. *In vitro*, significant D2 receptor internalization occurs within 5 to 10 min (Guo et al., 2010). Following amphetamine injection, raclopride displacement in mice lacking a protein required for internalization can be differentiated from wild-type mice at many hours, but not at about 1 h (Skinbjerg et al., 2010); however, the bolus approach used in the mouse study provides poor temporal information. In our study, the main feature of the PET data is the slow rate of apparent displacement, rather than the displacement magnitude at the end of the study 1 h later.

Formally, dynamic internalization could be incorporated into the D1 and D2 components of the fMRI model by separating receptors into external and internal fractions, so that Eq. (6) is modified as

$$\frac{d\theta_{ext}(t)}{dt} = k_{OFF, ext}\left[(1 - \theta_{ext}(t) - \theta_{int}(t))\frac{\theta_{ext}(0)}{1 - \theta_{ext}(0) - \theta_{int}(0)}f(t) - \theta_{ext}(t)\right].$$
(14)

Within the fMRI model, internalization will exacerbate effects of receptor saturation by dynamically lowering the level of available receptors. If we presume that the rate of internalization increases with

the level of DA occupancy at each receptor sub-type, then the higher affinity of DA for D2 receptors could lead to a more rapid or pronounced down-regulation of synaptic D2 receptors relative to D1 receptors. These issues require further investigation across a wider dose range, possibly using targeted exogenous agonists to simplify the description of the fMRI data.

Conclusions

This study developed a first-order multi-receptor model of DA-induced fMRI signal and showed that this model is capable of consistently describing a wide range of literature results. Within the model, fMRI signal arises from competing excitatory and inhibitory influences of D1 and D2 receptor stimulation, respectively, so that the net functional output depends upon relative receptor densities, affinities, and the level of evoked DA. In specific regimes, the model supports empirical observations that the temporal evolution of fMRI signal in basal ganglia closely matches the response of DA. More generally, however, evoked DA and fMRI signal diverge in the time domain, and DA-induced fMRI responses – both measured and modeled – can be negative, positive, or biphasic in nature. However, the model predicts predominantly negative DA-induced fMRI signal responses in human and NHP basal ganglia, except at very high levels of evoked DA.

When PET ^{11}C-raclopride data were measured simultaneously with fMRI responses to amphetamine in NHP, results suggested that DA-induced displacement of PET ligand occurred slowly in relation to the evolution of fMRI signal. Thus, it is reasonable to conclude that modification to the current model will be required to describe effects of dynamic receptor trafficking at high levels of agonist occupancy. fMRI and PET models of dopaminergic release and function possess many commonalities but reflect the underlying biological processes in different ways, so that combined measurements should inform our understanding of functional physiology.

Acknowledgments

Conflict of interest statement

The authors declare that there are no conflicts of interest.

References

Abi-Dargham, A., Rodenhiser, J., Printz, D., Zea-Ponce, Y., Gil, R., Kegeles, L.S., Weiss, R., Cooper, T.B., Mann, J.J., Van Heertum, R.L., Gorman, J.M., Laruelle, M., 2000. Increased baseline occupancy of D2 receptors by dopamine in schizophrenia. Proc. Natl. Acad. Sci. U. S. A. 97, 8104–8109.

Alpert, N.M., Badgaiyan, R.D., Livni, E., Fischman, A.J., 2003. A novel method for noninvasive detection of neuromodulatory changes in specific neurotransmitter systems. NeuroImage 19, 1049–1060.

Attwell, D., Laughlin, S.B., 2001. An energy budget for signaling in the grey matter of the brain. J. Cereb. Blood Flow Metab. 21, 1133–1145.

Bradberry, C.W., 2000. Acute and chronic dopamine dynamics in a nonhuman primate model of recreational cocaine use. J. Neurosci. 20, 7109–7115.

Carlezon Jr., W.A., Duman, R.S., Nestler, E.J., 2005. The many faces of CREB. Trends Neurosci. 28, 436–445.

Carson, R.E., Channing, M.A., Blasberg, R.G., Dunn, B.B., Cohen, R.M., Rice, K.C., Herscovitch, P., 1993. Comparison of bolus and infusion methods for receptor quantitation: application to [18F]cyclofoxy and positron emission tomography. J. Cereb. Blood Flow Metab. 13, 24–42.

Chen, Y.I., Brownell, A.L., Galpern, W., Isacson, O., Bogdanov, M., Beal, M.F., Livni, E., Rosen, B.R., Jenkins, B.G., 1999. Detection of dopaminergic cell loss and neural transplantation using pharmacological MRI, PET and behavioral assessment. Neuroreport 10, 2881–2886.

Chen, Y.C., Choi, J.K., Andersen, S.L., Rosen, B.R., Jenkins, B.G., 2005. Mapping dopamine D2/D3 receptor function using pharmacological magnetic resonance imaging. Psychopharmacology (Berl) 180, 705–715.

Chen, Y.I., Choi, J.K., Xu, H., Ren, J., Andersen, S.L., Jenkins, B.G., 2010. Pharmacologic neuroimaging of the ontogeny of dopamine receptor function. Dev. Neurosci. 32, 125–138.

Chen, Y.I., Famous, K., Xu, H., Choi, J.K., Mandeville, J.B., Schmidt, H.D., Pierce, R.C., Jenkins, B.G., 2011. Cocaine self-administration leads to alterations in temporal responses to cocaine challenge in limbic and motor circuitry. Eur. J. Neurosci. 34, 800–815.

Choi, J.K., Chen, Y.I., Hamel, E., Jenkins, B.G., 2006. Brain hemodynamic changes mediated by dopamine receptors: role of the cerebral microvasculature in dopamine-mediated neurovascular coupling. NeuroImage 30, 700–712.

Chou, Y.H., Karlsson, P., Halldin, C., Olsson, H., Farde, L., 1999. A PET study of D(1)-like dopamine receptor ligand binding during altered endogenous dopamine levels in the primate brain. Psychopharmacology (Berl) 146, 220–227.

Clark, A.J., 1937. General Pharmacology. Verlag von Julius Springer, Berlin 61–98 (176–206, 215–217).

Couppis, M.H., Kennedy, C.H., Stanwood, G.D., 2008. Differences in aggressive behavior and in the mesocorticolimbic DA system between A/J and BALB/cJ mice. Synapse 62, 715–724.

Cumming, P., 2011. Absolute abundances and affinity states of dopamine receptors in mammalian brain: a review. Synapse 65, 892–909.

Delforge, J., Bottlaender, M., Pappata, S., Loc'h, C., Syrota, A., 2001. Absolute quantification by positron emission tomography of the endogenous ligand. J. Cereb. Blood Flow Metab. 21, 613–630.

Endres, C.J., Kolachana, B.S., Saunders, R.C., Su, T., Weinberger, D., Breier, A., Eckelman, W.C., Carson, R.E., 1997. Kinetic modeling of [11C]raclopride: combined PET–microdialysis studies. J. Cereb. Blood Flow Metab. 17, 932–942.

Farde, L., Ehrin, E., Eriksson, L., Greitz, T., Hall, H., Hedstrom, C.G., Litton, J.E., Sedvall, G., 1985. Substituted benzamides as ligands for visualization of dopamine receptor binding in the human brain by positron emission tomography. Proc. Natl. Acad. Sci. U. S. A. 82, 3863–3867.

Frank, S.T., Krumm, B., Spanagel, R., 2008. Cocaine-induced dopamine overflow within the nucleus accumbens measured by in vivo microdialysis: a meta-analysis. Synapse 62, 243–252.

Ginovart, N., 2005. Imaging the dopamine system with in vivo [11C]raclopride displacement studies: understanding the true mechanism. Mol. Imaging Biol. 7, 45–52.

Ginovart, N., Farde, L., Halldin, C., Swahn, C.G., 1997. Effect of reserpine-induced depletion of synaptic dopamine on [11C]raclopride binding to D2-dopamine receptors in the monkey brain. Synapse 25, 321–325.

Gozzi, A., Ceolin, L., Schwarz, A., Reese, T., Bertani, S., Crestan, V., Bifone, A., 2007. A multimodality investigation of cerebral hemodynamics and autoregulation in pharmacological MRI. Magn. Reson. Imaging 25, 826–833.

Grubb, R.L., Phelps, M.E., Raichle, M.E., Ter-Pogossian, M.M., 1973. The effects of arterial blood pressure on the regional cerebral blood volume by X-ray fluorescence. Stroke 4, 390–399.

Guo, N., Hwang, D.R., Lo, E.S., Huang, Y.Y., Laruelle, M., Abi-Dargham, A., 2003. Dopamine depletion and in vivo binding of PET D1 receptor radioligands: implications for imaging studies in schizophrenia. Neuropsychopharmacology 28, 1703–1711.

Guo, N., Guo, W., Kralikova, M., Jiang, M., Schieren, I., Narendran, R., Slifstein, M., Abi-Dargham, A., Laruelle, M., Javitch, J.A., Rayport, S., 2010. Impact of D2 receptor internalization on binding affinity of neuroimaging radiotracers. Neuropsychopharmacology 35, 806–817.

Hall, H., Sedvall, G., Magnusson, O., Kopp, J., Halldin, C., Farde, L., 1994. Distribution of D1- and D2-dopamine receptors, and dopamine and its metabolites in the human brain. Neuropsychopharmacology 11, 245–256.

Hyttel, J., Arnt, J., 1987. Characterization of binding of 3H-SCH 23390 to dopamine D-1 receptors. Correlation to other D-1 and D-2 measures and effect of selective lesions. J. Neural Transm. 68, 171–189.

Ichise, M., Liow, J.S., Lu, J.Q., Takano, A., Model, K., Toyama, H., Suhara, T., Suzuki, K., Innis, R.B., Carson, R.E., 2003. Linearized reference tissue parametric imaging methods: application to [11C]DASB positron emission tomography studies of the serotonin transporter in human brain. J. Cereb. Blood Flow Metab. 23, 1096–1112.

Jenkins, B.G., Sanchez-Pernaute, R., Brownell, A.L., Chen, Y.C., Isacson, O., 2004. Mapping dopamine function in primates using pharmacologic magnetic resonance imaging. J. Neurosci. 24, 9553–9560.

Johnson, B., Lamki, L., Fang, B., Barron, B., Wagner, L., Wells, L., Kenny, P., Overton, D., Dhother, S., Abramson, D., Chen, R., Kramer, L., 1998. Demonstration of dose-dependent global and regional cocaine-induced reductions in brain blood flow using a novel approach to quantitative single photon emission computerized tomography. Neuropsychopharmacology 18, 377–384.

Kaufman, M.J., Levin, J.M., Maas, L.C., Rose, S.L., Lukas, S.E., Mendelson, J.H., Cohen, B.M., Renshaw, P.F., 1998. Cocaine decreases relative cerebral blood volume in humans: a dynamic susceptibility contrast magnetic resonance imaging study. Psychopharmacology (Berl) 138, 76–81.

Kirkland Henry, P., Davis, M., Howell, L.L., 2009. Effects of cocaine self-administration history under limited and extended access conditions on in vivo striatal dopamine neurochemistry and acoustic startle in rhesus monkeys. Psychopharmacology (Berl) 205, 237–247.

Kufahl, P.R., Li, Z., Risinger, R.C., Rainey, C.J., Wu, G., Bloom, A.S., Li, S.J., 2005. Neural responses to acute cocaine administration in the human brain detected by fMRI. NeuroImage 28, 904–914.

Lammertsma, A.A., Hume, S.P., 1996. Simplified reference tissue model for PET receptor studies. NeuroImage 4, 153–158.

Laruelle, M., 2000. Imaging synaptic neurotransmission with in vivo binding competition techniques: a critical review. J. Cereb. Blood Flow Metab. 20, 423–451.

Laruelle, M., D'Souza, C.D., Baldwin, R.M., Abi-Dargham, A., Kanes, S.J., Fingado, C.L., Seibyl, J.P., Zoghbi, S.S., Bowers, M.B., Jatlow, P., Charney, D.S., Innis, R.B., 1997a. Imaging D2 receptor occupancy by endogenous dopamine in humans. Neuropsychopharmacology 17, 162–174.

Laruelle, M., Iyer, R.N., al-Tikriti, M.S., Zea-Ponce, Y., Malison, R., Zoghbi, S.S., Baldwin, R.M., Kung, H.F., Charney, D.S., Hoffer, P.B., Innis, R.B., Bradberry, C.W., 1997b. Microdialysis and SPECT measurements of amphetamine-induced dopamine release in nonhuman primates. Synapse 25, 1–14.

Liu, C.H., Greve, D.N., Dai, G., Marota, J.J., Mandeville, J.B., 2007. Remifentanil administration reveals biphasic phMRI temporal responses in rat consistent with dynamic receptor regulation. NeuroImage 34, 1042–1053.

Logan, J., Dewey, S.L., Wolf, A.P., Fowler, J.S., Brodie, J.D., Angrist, B., Volkow, N.D., Gatley, S.J., 1991. Effects of endogenous dopamine on measures of [18F]N-methylspiroperidol binding in the basal ganglia: comparison of simulations and experimental results from PET studies in baboons. Synapse 9, 195–207.

London, E.D., Cascella, N.G., Wong, D.F., Phillips, R.L., Dannals, R.F., Links, J.M., Herning, R., Grayson, R., Jaffe, J.H., Wagner, H.N., 1990. Cocaine-induced reduction of glucose utilization in human brain. Arch. Gen. Psychiatry 47, 567–574.

Lyons, D., Friedman, D.P., Nader, M.A., Porrino, L.J., 1996. Cocaine alters cerebral metabolism within the ventral striatum and limbic cortex of monkeys. J. Neurosci. 16, 1230–1238.

Madras, B.K., Fahey, M.A., Canfield, D.R., Spealman, R.D., 1988. D1 and D2 dopamine receptors in caudate–putamen of nonhuman primates (Macaca fascicularis). J. Neurochem. 51, 934–943.

Mandeville, J.B., 2012. IRON fMRI measurements of CBV and implications for BOLD signal. NeuroImage 62, 1000–1008.

Mandeville, J.B., Choi, J.K., Jarraya, B., Rosen, B.R., Jenkins, B.G., Vanduffel, W., 2011. FMRI of cocaine self-administration in macaques reveals functional inhibition of basal ganglia. Neuropsychopharmacology 36, 1187–1198.

Mandeville, J.B., Sander, C.Y., Jenkins, B.G., Rosen, B.R., Hooker, J.M., Catana, C., Vanduffel, W., Alpert, N.M., Normandin, M.D., 2012. A Model of Dopamine-induced fMRI Response Informed by Simultaneous PET/fMRI. International Society of Magnetic Resonance and Medicine, Melbourne 2845.

Marcellino, D., Daniel, K., Jan, A., Luigi, F., Fuxe, K., 2011. Increased affinity of dopamine for D(2)-like versus D(1)-like receptors. Relevance for volume transmission in interpreting PET findings. Synapse (Epub ahead of print).

Marota, J.J.A., Mandeville, J.B., Weisskoff, R.M., Moskowitz, M.A., Rosen, B.R., Kosofsky, B.E., 2000. Cocaine activation discriminates dopaminergic projections by temporal response: an fMRI study in rat. NeuroImage 11, 13–23.

Martinez, D., Narendran, R., Foltin, R.W., Slifstein, M., Hwang, D.R., Broft, A., Huang, Y., Cooper, T.B., Fischman, M.W., Kleber, H.D., Laruelle, M., 2007. Amphetamine-induced dopamine release: markedly blunted in cocaine dependence and predictive of the choice to self-administer cocaine. Am. J. Psychiatry 164, 622–629.

Martinez, D., Greene, K., Broft, A., Kumar, D., Liu, F., Narendran, R., Slifstein, M., Van Heertum, R., Kleber, H.D., 2009. Lower level of endogenous dopamine in patients with cocaine dependence: findings from PET imaging of D(2)/D(3) receptors following acute dopamine depletion. Am. J. Psychiatry 166, 1170–1177.

McLaren, D.G., Kosmatka, K.J., Oakes, T.R., Kroenke, C.D., Kohama, S.G., Matochik, J.A., Ingram, D.K., Johnson, S.C., 2009. A population-average MRI-based atlas collection of the rhesus macaque. NeuroImage 45, 52–59.

Michaelis, L., Menten, M.L., Johnson, K.A., Goody, R.S., 2011. The original Michaelis constant: translation of the 1913 Michaelis–Menten paper. Biochemistry 50, 8264–8269.

Narendran, R., Hwang, D.R., Slifstein, M., Hwang, Y., Huang, Y., Ekelund, J., Guillin, O., Scher, E., Martinez, D., Laruelle, M., 2005. Measurement of the proportion of D2 receptors configured in state of high affinity for agonists in vivo: a positron emission tomography study using [11C]N-propyl-norapomorphine and [11C]raclopride in baboons. J. Pharmacol. Exp. Ther. 315, 80–90.

Nelissen, K., Jarraya, B., Arsenault, J., Rosen, B.R., Wald, L.L., Mandeville, J.B., Marota, J.J., Vanduffel, W., 2012. Neural correlates of the formation and retention of cocaine-induced stimulus–reward associations. Biol. Psychiatry 72, 422–428.

Neves, S.R., Ram, P.T., Iyengar, R., 2002. G protein pathways. Science 296, 1636–1639.

Normandin, M.D., Morris, E.D., 2008. Estimating neurotransmitter kinetics with ntPET: a simulation study of temporal precision and effects of biased data. NeuroImage 39, 1162–1179.

Normandin, M.D., Sander, C.Y., Catana, C., Hooker, J.M., Jenkins, B.G., Vanduffel, W., El Fakhri, G., Rosen, B.R., Alpert, N.M., Mandeville, J.B., 2012a. A kinetic model for mapping dopamine function with simultaneous PET/MR. NeuroReceptor Mapping Conference, Baltimore.

Normandin, M.D., Schiffer, W.K., Morris, E.D., 2012b. A linear model for estimation of neurotransmitter response profiles from dynamic PET data. NeuroImage 59, 2689–2699.

Pappata, S., Dehaene, S., Poline, J.B., Gregoire, M.C., Jobert, A., Delforge, J., Frouin, V., Bottlaender, M., Dolle, F., Di Giambernardino, L., Syrota, A., 2002. In vivo detection of striatal dopamine release during reward: a PET study with [(11)C]raclopride and a single dynamic scan approach. NeuroImage 16, 1015–1027.

Perles-Barbacaru, T.A., Procissi, D., Demyanenko, A.V., Hall, F.S., Uhl, G.R., Jacobs, R.E., 2011. Quantitative pharmacologic MRI: mapping the cerebral blood volume response to cocaine in dopamine transporter knockout mice. NeuroImage 55, 622–628.

Piggott, M.A., Marshall, E.F., Thomas, N., Lloyd, S., Court, J.A., Jaros, E., Costa, D., Perry, R.H., Perry, E.K., 1999. Dopaminergic activities in the human striatum: rostrocaudal gradients of uptake sites and of D1 and D2 but not of D3 receptor binding or dopamine. Neuroscience 90, 433–445.

Porrino, L.J., 1993. Functional consequences of acute cocaine treatment depend on route of administration. Psychopharmacology 112, 343–351.

Qiu, D., Zaharchuk, G., Christen, T., Ni, W.W., Moseley, M.E., 2012. Contrast-enhanced functional blood volume imaging (CE-fBVI): enhanced sensitivity for brain activation

in humans using the ultrasmall superparamagnetic iron oxide agent ferumoxytol. NeuroImage 62, 1726–1731.

Ren, J., Xu, H., Choi, J.K., Jenkins, B.G., Chen, Y.I., 2009. Dopaminergic response to graded dopamine concentration elicited by four amphetamine doses. Synapse 63, 764–772.

Risinger, R.C., Salmeron, B.J., Ross, T.J., Amen, S.L., Sanfilipo, M., Hoffmann, R.G., Bloom, A.S., Garavan, H., Stein, E.A., 2005. Neural correlates of high and craving during cocaine self-administration using BOLD fMRI. NeuroImage 26, 1097–1108.

Saleem, K.S., Logothetis, N.K., 2006. A Combined MRI and Histology Atlas of the Rhesus Monkey Brain. Academic Press, London, UK.

Sander, C.Y., Hooker, J.M., Catana, C., Normandin, M.D., Vanduffel, W., Rosen, B.R., Mandeville, J.B., 2012. Coupling of neurovascular response and receptor occupancy with simultaneous PET/fMRI. The 9th International Symposium on Functional Neuroreceptor Mapping of the Living Brain (NRM12), Baltimore.

Schmand, M., Burbar, Z., Corbeil, J.L., Zhang, N., Michael, C., Byars, L., Ericksson, L., 2007. Brain PET: first human tomograph for simultaneous (functional) PET and MR imaging. J. Nucl. Med. 48 (45P).

Schoffelmeer, A.N., Hogenboom, F., Mulder, A.H., Ronken, E., Stoof, J.C., Drukarch, B., 1994. Dopamine displays an identical apparent affinity towards functional dopamine D1 and D2 receptors in rat striatal slices: possible implications for the regulatory role of D2 receptors. Synapse 17, 190–195.

Schwarz, A.J., Zocchi, A., Reese, T., Gozzi, A., Garzotti, M., Varnier, G., Curcuruto, O., Sartori, I., Girlanda, E., Biscaro, B., Crestan, V., Bertani, S., Heidbreder, C., Bifone, A., 2004. Concurrent pharmacological MRI and in situ microdialysis of cocaine reveal a complex relationship between the central hemodynamic response and local dopamine concentration. NeuroImage 23, 296–304.

Seeman, P., 1987. The absolute density of neurotransmitter receptors in the brain. Example for dopamine receptors. J. Pharmacol. Methods 17, 347–360.

Skinbjerg, M., Liow, J.S., Seneca, N., Hong, J., Lu, S., Thorsell, A., Heilig, M., Pike, V.W., Halldin, C., Sibley, D.R., Innis, R.B., 2010. D2 dopamine receptor internalization prolongs the decrease of radioligand binding after amphetamine: a PET study in a receptor internalization-deficient mouse model. NeuroImage 50, 1402–1407.

Skinbjerg, M., Sibley, D.R., Javitch, J.A., Abi-Dargham, A., 2012. Imaging the high-affinity state of the dopamine D2 receptor in vivo: fact or fiction? Biochem. Pharmacol. 83, 193–198.

Sokoloff, P., Martres, M.P., Giros, B., Bouthenet, M.L., Schwartz, J.C., 1992. The third dopamine receptor (D3) as a novel target for antipsychotics. Biochem. Pharmacol. 43, 659–666.

Stoof, J.C., Kebabian, J.W., 1981. Opposing roles for D-1 and D-2 dopamine receptors in efflux of cyclic AMP from rat neostriatum. Nature 294, 366–368.

Thompson, D., Martini, L., Whistler, J.L., 2010. Altered ratio of D1 and D2 dopamine receptors in mouse striatum is associated with behavioral sensitization to cocaine. PLoS One 5, e11038.

Trugman, J.M., James, C.L., 1993. D1 dopamine agonist and antagonist effects on regional cerebral glucose utilization in rats with intact dopaminergic innervation. Brain Res. 607, 270–274.

Verhoeff, N.P., Kapur, S., Hussey, D., Lee, M., Christensen, B., Psych, C., Papatheodorou, G., Zipursky, R.B., 2001. A simple method to measure baseline occupancy of neostriatal dopamine D2 receptors by dopamine in vivo in healthy subjects. Neuropsychopharmacology 25, 213–223.

Verhoeff, N.P., Hussey, D., Lee, M., Tauscher, J., Papatheodorou, G., Wilson, A.A., Houle, S., Kapur, S., 2002. Dopamine depletion results in increased neostriatal D(2), but not D(1), receptor binding in humans. Mol. Psychiatry 7 (233), 322–328.

Volkow, N.D., Fowler, J.S., Wang, G.-J., Hitzemann, R., Logan, J., Schlyer, D.J., Dewey, S.L., Wolf, A.P., 1993. Decreased dopamine D2 receptor availability is associated with reduced frontal metabolism in cocaine abusers. Synapse 14, 169–177.

Wallace, E.A., Wisniewski, G., Zubal, G., vanDyck, C.H., Pfau, S.E., Smith, E.O., Rosen, M.I., Sullivan, M.C., Woods, S.W., Kosten, T.R., 1996. Acute cocaine effects on absolute cerebral blood flow. Psychopharmacology (Berl) 128, 17–20.

Weed, M.R., Woolverton, W.L., Paul, I.A., 1998. Dopamine D1 and D2 receptor selectivities of phenyl-benzazepines in rhesus monkey striata. Eur. J. Pharmacol. 361, 129–142.

Wilson, S.J., Sayette, M.A., Fiez, J.A., 2004. Prefrontal responses to drug cues: a neurocognitive analysis. Nat. Neurosci. 7, 211–214.

Zaharchuk, G., Mandeville, J.B., Bogdonov Jr., A.A., Weissleder, R., Rosen, B.R., Marota, J.J.A., 1999. Cerebrovascular dynamics of autoregulation and hypotension: an MRI study of CBF and changes in total and microvascular cerebral blood volume during hemorrhagic hypotension. Stroke 30, 2197–2205.

Zocchi, A., Conti, G., Orzi, F., 2001. Differential effects of cocaine on local cerebral glucose utilization in the mouse and in the rat. Neurosci. Lett. 306, 177–180.